β-detected nuclear quadrupole resonance with a low-energy beam of $^8Li^+$

Z. Salman,[1] E. P. Reynard,[1] W. A. MacFarlane,[2] K. H. Chow,[3] J. Chakhalian,[1,4] S. R. Kreitzman,[1] S. Daviel,[1] C. D. P. Levy,[1] R. Poutissou,[1] and R. F. Kiefl[1,4,5]

[1]*TRIUMF, 4004 Wesbrook Mall, Vancouver, British Columbia, Canada V6T 2A3*

[2]*Chemistry Department, University of British Columbia, Vancouver, British Columbia, Canada V6T 1Z1*

[3]*Department of Physics, University of Alberta, Edmonton, Alberta, Canada T6G 2J1*

[4]*Department of Physics and Astronomy, University of British Columbia, Vancouver, British Columbia, Canada V6T 1Z1*

[5]*Canadian Institute for Advanced Research, Toronto, Ontario, Canada M5G 1Z8*

(Received 1 December 2003; revised manuscript received 11 May 2004; published 9 September 2004)

A nuclear quadrupole resonance (NQR) spectrum of ^8Li has been observed in a single crystal of $SrTiO_3$ using a beam of low-energy highly polarized radioactive $^8Li^+$. The resonances were detected by monitoring the β-decay anisotropy as a function of a small audio frequency magnetic field. These results demonstrate that low energy nuclear spin polarized ^8Li can be used as a sensitive probe of the local magnetic and electronic environment in nanostructures and ultrathin films in zero static applied magnetic field.

DOI: 10.1103/PhysRevB.70.104404 PACS number(s): 83.85.−c, 76.60.Gv, 76.75.+i

I. INTRODUCTION

Nuclear magnetic resonance (NMR) and nuclear quadrupole resonance (NQR) are powerful techniques for probing the local electric/magnetic properties of materials. Since one requires a large number (10^{20}) of nuclear spins in order to generate a signal, these methods are most widely used in studies of bulk materials.[1] However, much greater sensitivity can be obtained with closely related nuclear methods such as β-detected nuclear magnetic resonance (β-NMR) where the signal comes from the decay properties of a radioactive nucleus.[2–5] For example, in the case of ^8Li, which has a mean lifetime of 1.2 s, a high energy electron is emitted preferentially in the opposite direction of the nuclear polarization. We have recently created a beam of low-energy highly polarized radioactive $^8Li^+$ for doing β-NMR.[5] Since only about 10^7 spins are needed to generate a signal, β-NMR is well suited for studies of dilute impurities, nanostructures or ultrathin films where there are a few host nuclear spins.

In this paper we show that it is also possible to perform β-detected nuclear quadrupole resonance (β-NQR) in zero magnetic field. The β-NQR spectrum was obtained for ^8Li implanted into a single crystal of $SrTiO_3$ in zero field. The ability to perform depth profiling measurements on a nm scale in zero magnetic field has many potential applications in studies of magnetism and superconductivity. It is also remarkable that the resonances are narrow (few kHz) and easily observed at acoustic frequencies. Recall that in conventional NQR the signal to noise ratio degrades rapidly with decreasing frequency, and has a lower limit of a few MHz.

β-NMR has close similarities to both muon spin rotation and conventional NMR. In all forms of nuclear magnetic resonance one typically produces nuclear polarization out of equilibrium and then observes how that polarization evolves in time. The two basic observables are the spin precession and relaxation rates, which are sensitive to the local electric/magnetic environment. β-NMR is carried out by applying a static external magnetic field (B) along the initial spin polarization direction. A small oscillating magnetic field (B_1) is applied perpendicular to the nuclear polarization and is stepped through a range of frequencies around the Larmor frequency. A resonant loss of polarization occurs when the frequency of B_1 matches the Larmor frequency of the nucleus. β-NQR is performed in the absence of a static magnetic field ($B=0$). It is well known that if a nucleus with an electric quadrupole moment rests in a crystalline site with noncubic symmetry, there will be a quadrupolar splitting of the nuclear spin levels even in zero external field. One can induce transitions between these levels with a transverse oscillating magnetic field (B_1) and thereby alter the nuclear spin population. In the case of ^8Li the resulting quadrupolar resonances occur typically at acoustic frequencies. The results presented here demonstrate that a low-energy polarized beam of ^8Li can be used as a sensitive probe of the magnetic properties in zero external field. Since the implantation energy is adjustable we anticipate that one can obtain such information as a function of depth on a nanometer scale.[6]

II. EXPERIMENTAL

A. Polarized ^8Li beam

The experiment was performed at the TRIUMF ISAC facility where a 500 MeV proton beam is used for production of radioactive ions. A wide variety of isotopes are released from the surface ionization source heated to 2000 °C but alkali are preferentially ionized because of their low ionization energy. The resulting positive ions are extracted from the target and then accelerated to 30 keV to form a low emittance beam with an energy spread of 1–2 eV. The beam is then passed through a high resolution mass spectrometer so that only the isotope of interest reaches the experimental area. A more complete description of the ISAC facility may be found elsewhere.[7]

Although many isotopes can be generated at ISAC, ^8Li is the lightest one suitable for β-NMR. The main criteria for both β-NMR or β-NQR are that the production rate from the source is high and that the beam can be easily polarized.

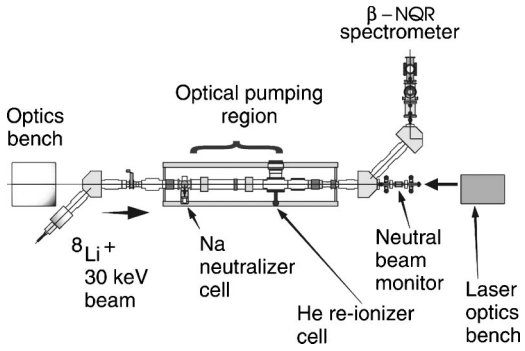

FIG. 1. A schematic of the experimental layout. The 30 keV $^8Li^+$ ion beam is neutralized in the Na cell and then reionized in the He cell. In between, the beam is optically pumped with a laser tuned to the D1 optical transition of the ^{8}Li atom. The resulting polarized ion beam is guided to the β-NQR spectrometer.

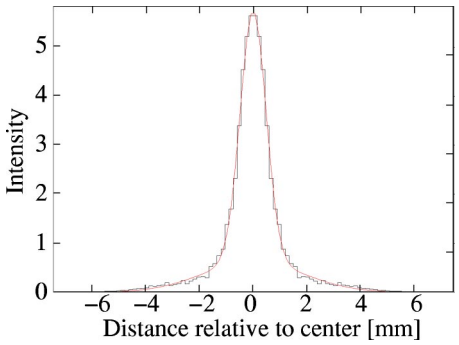

FIG. 2. Profile of the ^{8}Li beam stopping in a plastic scintillator taken from a CCD image of the beam. The solid line is a fit of the profile to a Lorentzian shape.

^{8}Li ($I=2$) satisfies these criteria and has many other properties that are suitable for both these techniques. It is a light ion, so the vast majority of the implanted Li ends up in well-defined crystalline sites. Also the mean lifetime (1.2 s) is comparable to typical spin relaxation times in many materials. Both the gyromagnetic ratio ($\gamma=6.3$ MHz/T) and electric quadrupole moment of ^{8}Li ($Q=33$ mB) are small so that hyperfine interactions with the crystal environment are weak. For example, in metals we expect small Knight shifts (in the 100 ppm range); whereas, the electric quadrupolar splittings at noncubic sites should be in the 10's of kHz range. Thus, with narrow resonances and relaxation rates slow compared to heavier nuclei, ^{8}Li can act as a high resolution probe of internal magnetic fields in solids.

Large nuclear polarization of the low-energy $^8Li^+$ beam is created using a fast collinear optical pumping method which is well established for the case of alkalis.[8] A layout of the polarizer showing the location of the NQR spectrometer is shown in Fig. 1.

Circular polarized light from a single frequency ring dye laser (300 mW CW power) is directed along the beam axis.[9] The first step in the procedure is to neutralize the ion beam by passing it through a Na vapor cell. The neutral beam then drifts 1.9 m in the optical pumping region in the presence of a small (1 mT) longitudinal magnetic field. The D1 atomic transition $2s\ ^2S_{1/2} \rightarrow 2p\ ^2P_{1/2}$ of neutral Li occurs at 671 nm. After about 10–20 cycles of absorption and spontaneous emission, a high degree of electronic and nuclear spin polarization is achieved. The final step is to strip off the valence electron by passing it through a He gas cell.[10] The polarized $^8Li^+$ beam can then be guided electrostatically into the spectrometer without affecting the nuclear spin polarization. Typically the polarization of the beam is about 70% and very stable on the time scale of a measurement. Since the spectrometer is oriented at 90 degrees to the polarizer (see Fig. 1) the beam enters the spectrometer with transverse polarization.

The final electrostatic elements of the beamline are used to focus and steer the beam to the sample. This tuning is achieved by placing a plastic scintillator at the sample position and viewing it with a CCD camera through a quartz window downstream of the sample. ^{8}Li decays to ^{8}Be which in turn promptly decays into two energetic alphas of 1–2 MeV. The resulting light emitted from the scintillator is imaged with the camera. A typical intensity profile of the image is shown in Fig. 2. The wings are attributed to light scattered within the scintillator; whereas, the sharp central peak is associated with the beam spot. More than 95% of the beam falls within a 4 mm diameter. This defines the minimum area of a sample that can be studied.

The nominal energy of the beam is 30 keV and corresponds to an average implantation depth of about 200 nm. However, we have recently demonstrated that it is possible to decelerate such a beam down to 100 eV or less by placing the spectrometer on a high voltage platform. Once such a system is installed on the β-NQR spectrometer it will be possible to measure the β-NQR signal as a function of implantation depth in the range 1–200 nm.

B. Spectrometer

A schematic of the β-NQR spectrometer is shown in Fig. 3. The $^8Li^+$ beam enters an ultrahigh vacuum (UHV)

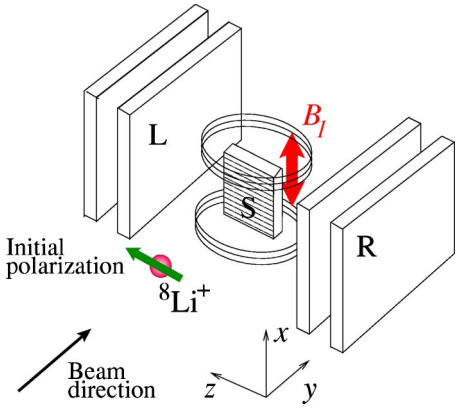

FIG. 3. A schematic of the spectrometer for β-detected nuclear quadrupole resonance. The spin polarization is perpendicular to the beam direction and the oscillating B_1 magnetic field. The principal axis of the electric field gradient at the Li stopping site must have a component along $\hat{z}$ in order for a signal to be detected at zero applied field.

chamber (not shown) and is focussed onto the sample. A small coil in an approximately Helmholtz configuration is used to apply an oscillating magnetic field (B_1) at frequency ν in the vertical direction, perpendicular to both the beam and initial polarization. The coil consists of six loops of Cu wire on a 16 mm radius. In the measurements described below the amplitude of B_1 was about 0.1 mT. The β's from decay of ^{8}Li have a mean energy of about 6 MeV which is enough to easily pass through thin stainless steel windows (0.05 mm thick) out of the UHV chamber and reach the detectors labelled *L* and *R*. Each detector telescope consists of a pair of BC 412 plastic scintillators measuring 10 cm $\times$10 cm$\times$0.3 cm thick located outside the UHV chamber. A set of three magnetic coils are present which allow one to apply a static uniform magnetic field (0–15 mT along the initial polarization direction or to zero at the field to within 0.005 mT.

Electron events are counted at each B_1 frequency ν. The time averaged nuclear polarization along the $\hat{z}$ direction (P_z) is directly proportional to the β-decay asymmetry,

$$AP_z(\nu) = \frac{L(\nu) - R(\nu)}{L(\nu) + R(\nu)}, \tag{1}$$

where $L(\nu)$ and $R(\nu)$ are the number of counts in the left and right detectors at frequency ν (corrected for the slightly different efficiencies of the detectors by reversing the initial polarization direction). The proportionality constant $A \approx 0.15$ depends on the beam polarization, the β-decay characteristics, and various instrumental parameters. The β-NQR is detected by measuring the β-decay asymmetry in zero applied field as a function of ν (see Fig. 5). The signal is the time dependent polarization function $p_z(t,\nu)$ averaged over the Li lifetime τ_β,

$$P_z(\nu) = \frac{1}{\tau_\beta}\int_0^\infty \exp[-t/\tau_\beta]p_z(t,\nu)\mathrm{d}t, \tag{2}$$

where *t* is the time after arrival in the sample. Equation (2) takes into account that the ^{8}Li arrives randomly and decays over its radioactive lifetime. Resonant dips in time averaged signal $P_z(\nu)$ occur when ν is matched to a nuclear spin splitting subject to the usual magnetic dipole selection rule $\Delta m = \pm 1$. One must step through the resonance slowly so that there are no memory effects, since the signal can only respond to a change in the applied frequency on a time scale determined by the ^{8}Li lifetime.

III. THEORY

We expect that the implanted Li will reside at well-defined crystalline lattice sites which can be interstitial or substitutional. Each site with noncubic symmetry is characterized by an electric field gradient tensor (EFG) which couples to the electric quadrupole moment of ^{8}Li giving rise to a zero field (ZF) splitting of the nuclear spin levels.[11] These splittings and the resulting nuclear quadrupole resonance spectrum are thus a fingerprint of the Li site. Assuming the EFG tensor is axially symmetric about some axis *z*, the quadrupolar spin Hamiltonian is[1]

$$\mathcal{H}_q = \nu_q(I_z^2 - 2), \tag{3}$$

where $\nu_q = e^2qQ/8$, $eq = V_{zz}$ is the electric field gradient along the symmetry axis, and *Q* is the electric quadrupole moment of the nucleus. The energy eigenvalues $E_m = \nu_q(m^2-2)$ are a function of the azimuthal quantum number *m* where $I_z|m\rangle = m|m\rangle$. In zero applied field there are two possible resonant frequencies (for $I=2$) at ν_q and $3\nu_q$ corresponding to the allowed magnetic dipole transitions $0 \leftrightarrow \pm 1$ and $\pm 1 \leftrightarrow \pm 2$, respectively. The amplitude of each resonance is directly proportional to the induced change in the nuclear spin polarization $P_z(\nu)$ on resonance. For convenience, we define **p** to be a vector whose elements (p_m) are the probability for a particular *m* state to be occupied. The projection of the nuclear polarization measured along the *z* direction for a spin 2 nucleus is then

$$P_z(\nu) = \frac{1}{2}\sum_{m=-2}^{+2} p_m m. \tag{4}$$

For example, if the Li beam is fully polarized along the symmetry axis of the EFG then with B_1 off $\mathbf{p_m} = \langle 1,0,0,0,0\rangle$ so that the $P_z(\nu)=1$. When B_1 is on resonance at $3\nu_q$ the occupation probabilities for $m=2$ and $m=1$ states are quickly equalized so that $P_z(\nu)=3/4$. Thus at the $3\nu_q$ resonance we expect a normalized resonance amplitude of 0.25. In this ideal case the amplitude of the resonance at $\nu = \nu_q$ will be zero since the $m=\pm 1$ and $m=0$ states are unoccupied. Now consider an initial spin population vector $\mathbf{p} = \langle 2/3,1/3,0,0,0\rangle$ which corresponds to a polarization of 5/6, closer to the experimental value. After irradiating at $3\nu_q$ we expect a 10% drop in the polarization to 3/4 or a normalized resonance amplitude 0.10. Similarly the amplitude at ν_q will be 0.20.

This treatment of the amplitude neglects all effects due to small perturbations, such as stray magnetic fields or slight deviations in the quadrupolar interaction. In fact, such perturbations can have a surprisingly large effect on the β-NQR spectrum. This may be traced to the fact that in zero magnetic field the $|\pm m\rangle$ states are degenerate and therefore easily mixed.

Consider first a small magnetic field *B* which is oriented along *z*, the symmetry axis of the EFG. The resulting Zeeman interaction lifts the degeneracy between $|\pm m\rangle$ states in first order but does not mix the states since it commutes with $\mathcal{H}_q$. Although the resonance positions are shifted by a small amount there is no change in the amplitudes. For example, the resonance corresponding to the $+2 \rightarrow +1$ transition shifts by γB. On the other hand, if $B = B_x$ is applied in the *x* direction the Zeeman interaction does not commute with $\mathcal{H}_q$. Although the splitting of the $|\pm m\rangle$ states occurs only in second order, such a perturbation mixes the $\pm m$ levels and consequently has a dramatic effect on the nuclear polarization and amplitudes of the β-NQRs. Using perturbation theory one finds that the $|1\rangle$ and $|-1\rangle$ states are mixed in second order through the magnetic dipole coupling to $|0\rangle$. The true eigenstates $|1a\rangle$ and $|1s\rangle$ are a coherent mixture of the $|1\rangle$ and $|-1\rangle$ states with a characteristic frequency splitting

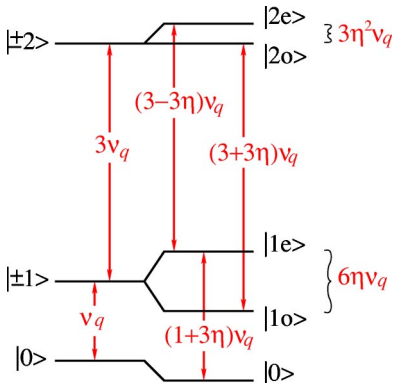

FIG. 4. The energy levels for $\mathcal{H}_q/h$ (left-hand side) and $(\mathcal{H}_q+\mathcal{H}_\eta)/h$ (right-hand side). The possible transitions induced by an oscillating field B_1 are also indicated.

$$\Delta_2 = \frac{2(\gamma B)^2\langle -1|I_x|0\rangle\langle 0|I_x|1\rangle}{E_1 - E_0} = \frac{3(\gamma B_x)^2}{\nu_q}. \tag{5}$$

The splitting of the resonance is small compared to B along z but the mixing of the m states implies that the B_1 indirectly connects $|2\rangle$ to $|-1\rangle$ (and subsequently to $|-2\rangle$) through $|1\rangle$. This in turn means the entire nuclear polarization is destroyed at the $3\nu_q$ resonance, provided Δ_2 is comparable to or larger than the ^{8}Li decay rate $(1/\tau_\beta)$. This corresponds to a dramatic increase in the amplitude of the resonance at $3\nu_q$ compared to the case with no m state mixing. At the same time, the resonance at ν_q is suppressed. Furthermore, even in the absence of B_1, any polarization associated with occupation of the $m=1$ state will oscillate at Δ_2. Note such a field will also mix the $|2\rangle$ and $|-2\rangle$ states but only in fourth order. However, any component of the external field along the symmetry axis will act to suppress the $|\pm m\rangle$ state mixing. In particular, the mixing is suppressed when the diagonal Zeeman interaction (γB_z) is large compared to Δ_2.

Another perturbation that can lead to $|\pm m\rangle$ state mixing is a nonaxial EFG resulting from, for example, crystal imperfections. Consider a small term which breaks the axial symmetry of the EFG,[11,12]

$$\mathcal{H}_\eta = \eta\nu_q(I_x^2 - I_y^2). \tag{6}$$

Here η is the conventional dimensionless EFG asymmetry parameter.[11,12] Exact diagonalization of the full Hamiltonian $\mathcal{H}_q+\mathcal{H}_\eta$ is presented in the Appendix. The energy level scheme of the full Hamiltonian for $\eta \ll 1$ is presented in Fig. 4, and shows that the $|1\rangle$ and $|-1\rangle$ states are mixed in first order. The true eigenstates $|1e\rangle$ and $|1o\rangle$ are a coherent mixture of the $|\pm 1\rangle$ states with characteristic frequency splitting

$$\Delta_1 = 6\eta\nu_q. \tag{7}$$

Even small values of η (e.g., 0.01) will produce strong mixing of the $m=\pm 1$ states and consequently a large increase in the amplitude of the resonance at $3\nu_q$. Such a term also leads to mixing of the $|\pm 2\rangle$ states in second order with a characteristic frequency splitting

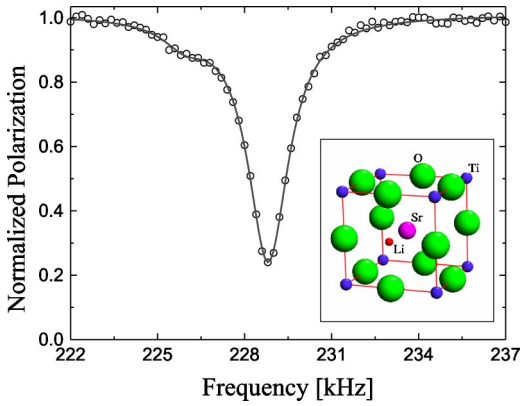

FIG. 5. The β-NQR spectrum obtained for a $SrTiO_3$ single crystal at room temperature and zero external field. Inset: The cubic unit cell of $SrTiO_3$ showing the proposed interstitial Li site at the face center.

$$\Delta_2 = 3\eta^2\nu_q. \tag{8}$$

Note however when η is small, mixing of the $|\pm 2\rangle$ states is much weaker than for the $|\pm 1\rangle$ states.

To summarize, the β-NQR amplitude is very sensitive to realistic small perturbations, as a consequence of the degeneracy of eigenstates of the (axially symmetric) quadrupolar Hamiltonian [Eq. (3)].

IV. RESULTS

The epitaxially polished $\langle 100\rangle$ single crystal of $SrTiO_3$ was purchased from Applied Technology Enterprises and had a RMS surface roughness of 1.5 Å.[13] A previous study showed a quadrupolar split $^8Li^+$ β-NMR resonance in $SrTiO_3$ in a large applied field of 3 T,[13] indicating that the Li resides in a site of noncubic symmetry. Properties of the high field β-NMR spectrum (position and amplitude of the quadrupole satellites) allowed us to conclude that the EFG principal axis z is parallel to a cubic axis. The most obvious noncubic candidate ^{8}Li site consistent with this is the face centered site (F) with EFG symmetry axis parallel to a cubic axis of the crystal (see inset of Fig. 5) with a quadrupolar frequency of $\nu_q \sim 76.6$ kHz.

Figure 5 shows the β-NQR spectra collected from the $SrTiO_3$. A large and sharp resonance was observed at $3\nu_q = 228.81(2)$ kHz with width 1.7 kHz corresponding to the $2 \leftrightarrow 1$ transition; whereas, the resonance near ν_q was barely visible.

Recall that the unperturbed Hamiltonian $\mathcal{H}_q$ [Eq. (3)] predicts a normalized amplitude of about 0.10, whereas the observed resonance amplitude is close to 0.8. This is strong evidence for an additional term in the spin Hamiltonian which mixes the $m=\pm 1$ states. This was confirmed by rotating the $\langle 100\rangle$ direction of the crystal away from the initial polarization direction by an angle θ, and measuring the polarization off resonance (without an oscillating magnetic field B_1). If there were no $|\pm m\rangle$ state mixing, the polarization would be independent of crystal orientation for a cubic lattice (see the dashed line in Fig. 6). However, the data show a

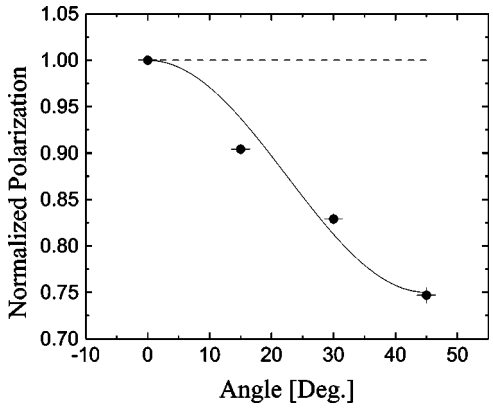

FIG. 6. The polarization as a function of the angle between the initial spin polarization and the ⟨100⟩ lattice direction.

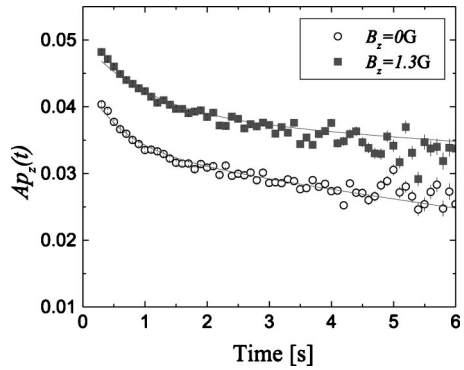

FIG. 7. The effect of small longitudinal field on the time dependence of ^{8}Li polarization as a function of time in $SrTiO_3$ at RT and no B_1.

clear drop in the polarization as one rotates the crystal 45 degrees, such that z is parallel to ⟨110⟩ direction.

The observed angular dependence is explained if one assumes the $m=\pm1$ states are rapidly mixed compared to the lifetime of ^{8}Li, so that the only contribution to the observed polarization is from the $m=\pm2$ states. This is calculated by taking the projection of the initial polarization on the $|\pm2\rangle$ states in the rotated EFG axis system, then taking the polarization component along the measurement axis z (solid line in Fig. 6),

$$p_z = \frac{1}{2}\cos(\theta)(2|\langle 2|e^{i\theta I_y}|2\rangle|^2 - 2|\langle -2|e^{i\theta I_y}|2\rangle|^2) + \frac{1}{2}\cos\left(\frac{\pi}{2}-\theta\right)(2|\langle 2|e^{-i[(\pi/2)-\theta]I_y}|2\rangle|^2 - 2|\langle -2|e^{-i[(\pi/2)-\theta]I_y}|2\rangle|^2). \quad (9)$$

Note that two equivalent F sites contribute to the polarization in this case.

The precise origin of the $|\pm m\rangle$ state mixing is not clear. However, it should be noted there are few host nuclear dipole moments in $SrTiO_3$. Furthermore, a careful zeroing of the external field had no influence on the amplitude of the resonance at $3\nu_q$, suggesting that the relevant perturbation is a small η or distribution of η's reflecting a slightly nonaxial EFG. Asymmetry parameters (η) as small as 0.01 could account for our observations. Such small values of η could arise from slight crystal imperfections, from intrinsic defects, or defects created by the implantation of ^{8}Li. It is also possible there is a slight disorder due to the close proximity to the surface. In such a situation, one would expect some off-axis component to the EFG due to the surface whose normal is perpendicular to the initial polarization direction and symmetry axis of the EFG. It is known that, in a metallic environment, the quadrupole frequency characteristic of a particular site recovers very quickly to its bulk value as one moves away from the surface.[14] However, the situation may be different in a high dielectric insulating medium such as $SrTiO_3$.

Note the resonance in Fig. 5 slightly asymmetric. The solid curve is a fit assuming two overlapping lines. The smaller amplitude line occurs at a slightly lower frequency $\nu=225.9(2)$ kHz and has a width of about 1.9(1) kHz which is similar to the higher frequency line at $\nu=228.8$ kHz. Both lines have a width which is three times greater than one would expect from B_1 power broadening. The splitting and finite linewidths, together with the $\pm m$ state mixing, are evidence for a distribution of slightly nonaxial EFG tensors. It is unclear if this distribution is intrinsic or caused by distant vacancies or interstitials generated by the Li implantation.

Time differential measurements of the nuclear polarization are carried out by delivering a short pulse of beam to the sample and observing the subsequent β decay asymmetry as a function of time, $p_z(t)$. Figure 7 shows the time evolution of the nuclear polarization in zero and a small longitudinal field (parallel to z) of 1.3 G, and without an oscillating magnetic field B_1.

Note that even this small magnetic field affects the initial amplitude of the polarization function. This is attributed to decoupling of the $|\pm1\rangle$ state mixing as one would expect if η were about 0.01. In addition, however, there is significant relaxation of the polarization which is not influenced by the small magnetic field. The form of the relaxation is well described by a sum of two exponentials. In zero field, the amplitude of the slow relaxing component was found to be equal to the amplitude of the main NQR line. This suggests that the main line in the β-NQR spectrum corresponds to the slow spin relaxation rate in Fig. 7 whereas the smaller resonance has the faster relaxation rate. Li diffusion or paraelectric fluctuations could cause such relaxation.[15] The temperature and magnetic field dependence is needed to resolve the origin of the relaxation.

In $SrTiO_3$ and related perovskite oxides, the mobility of interstitial Li is of interest in the context of ionic conductors.[16] Our observation of the characteristic NQR signal of Li in the F site of stoichiometric $SrTiO_3$, characterizes an important bottleneck state in the diffusive motion. It is likely that β-NQR will be a sensitive way to investigate the diffusive motion of isolated Li in such crystals.

V. SUMMARY AND CONCLUSION

We have demonstrated that it is possible to carry out β-detected nuclear quadrupole resonance using a beam of

low-energy highly polarized $^8Li^+$. Sharp β-NQRs were observed in $SrTiO_3$ indicating that the implanted Li adopts well-defined crystalline lattice sites. There is evidence for small nonaxial terms in the EFG tensor leading to mixing of the $\pm m$ states and a dramatic enhancement of the amplitude of the resonance at $3\nu_q$. Finally we mention that $SrTiO_3$ is not an isolated case. We have also observed β-NQRs in other compounds such as α-Al_2O_3 and metallic Sr_2RuO_4. We anticipate that the technique has many applications in studies of ultrathin films and interfaces. For example, in superconductors it could be used to measure the absolute value of the London penetration depth or to search for states with broken time reversal symmetry. In semiconductors or ionic compounds it can be used to study the diffusion and electronic structure of isolated Li in reduced geometries.

ACKNOWLEDGMENTS

This work was supported by the CIAR, NSERC, and TRIUMF. The authors thank Rahim Abasalti, Bassam Hitti, and Mel Good for technical support. The authors also thank Laura Greene for providing the $SrTiO_3$ sample.

APPENDIX

The Hamiltonian of spin $I=2$ at zero field in a nonaxial electric field gradient (EFG) is

$$\mathcal{H} = \nu_q[(I_z^2 - 2) + \eta(I_x^2 - I_y^2)] = \nu_q\left[(I_z^2 - 2) + \frac{\eta}{2}(I_+^2 + I_-^2)\right], \tag{A1}$$

where $\nu_q = e^2qQ/8$, $eq = V_{zz}$ is the EFG along the symmetry axis z, Q is the electric quadrupole moment of the nucleus, and η is the conventional dimensionless EFG asymmetry parameter.[11,12] In the presence of a transverse oscillating magnetic field, $\vec{B}_1(t) = \nu_1/\gamma\cos(2\pi\nu t)\hat{x}$, where $\gamma = 6.3$ MHz/T is the gyromagnetic ratio of the ^{8}Li nucleus, an additional term

$$\mathcal{H}_{RF} = \frac{\nu_1}{2}(I_+ + I_-)\cos(2\pi\nu t), \tag{A2}$$

is added to the Hamiltonian.

Let $|m\rangle$ be the eigenvectors of I_z with eigenvalues m. Taking even/odd representation basis

$$|2e\rangle = \frac{1}{\sqrt{2}}[|2\rangle + |-2\rangle],$$

$$|1e\rangle = \frac{1}{\sqrt{2}}[|1\rangle + |-1\rangle],$$

$$|0\rangle = |0\rangle,$$

$$|1o\rangle = \frac{1}{\sqrt{2}}[|1\rangle - |-1\rangle],$$

$$|2o\rangle = \frac{1}{\sqrt{2}}[|2\rangle - |-2\rangle], \tag{A3}$$

the full Hamiltonian matrix becomes

$$\begin{pmatrix} 2\nu_q & \nu_1\cos(2\pi\nu t) & \sqrt{12}\eta\nu_q & 0 & 0 \\ \nu_1\cos(2\pi\nu t) & (3\eta-1)\nu_q & \sqrt{3}\nu_1\cos(2\pi\nu t) & 0 & 0 \\ \sqrt{12}\eta\nu_q & \sqrt{3}\nu_1\cos(2\pi\nu t) & -2\nu_q & 0 & 0 \\ 0 & 0 & 0 & -(3\eta+1)\nu_q & \nu_1\cos(2\pi\nu t) \\ 0 & 0 & 0 & \nu_1\cos(2\pi\nu t) & 2\nu_q \end{pmatrix}, \tag{A4}$$

therefore even with $\nu_1 = 0$, if the initial spin state is with full polarization along $\hat{z}$, $|2\rangle$, half of the polarization is actually in the $|2o\rangle$ state while the other half is in the $|2e\rangle$ state. However, the $|2e\rangle$ is not an eigenstate of the Hamiltonian $\mathcal{H}$.

To diagonalize $\mathcal{H}$ we introduce the angle Γ, where $\tan(2\Gamma) = \sqrt{3}\eta$. Using the representation $|2e'\rangle$, $|1e\rangle$, $|0'\rangle$, $|1o\rangle$, and $|2o\rangle$, where (A5)

$$|2e'\rangle = \cos(\Gamma)|2e\rangle + \sin(\Gamma)|0\rangle, \quad |0'\rangle = \cos(\Gamma)|2e\rangle - \sin(\Gamma)|0\rangle, \tag{A5}$$

the full Hamiltonian is

$$\begin{pmatrix} 2\nu_q\sqrt{1+3\eta^2} & \alpha_{2e'\leftrightarrow 1e} & 0 & 0 & 0 \\ \alpha_{2e'\leftrightarrow 1e} & (3\eta-1)\nu_q & \alpha_{1e\leftrightarrow 0'} & 0 & 0 \\ 0 & \alpha_{1e\leftrightarrow 0'} & -2\nu_q\sqrt{1+3\eta^2} & 0 & 0 \\ 0 & 0 & 0 & -(3\eta+1)\nu_q & \alpha_{1o\leftrightarrow 2o} \\ 0 & 0 & 0 & \alpha_{1o\leftrightarrow 2o} & 2\nu_q \end{pmatrix}, \tag{A6}$$

where $\alpha_{i\leftrightarrow j}$ are the transition amplitudes from the eigenstate $|i\rangle$ to $|j\rangle$,

$$\alpha_{2e'\leftrightarrow 1e} = \nu_1[\cos(\Gamma) + \sqrt{3}\sin(\Gamma)]\cos(2\pi\nu t),$$

$$\alpha_{1e\leftrightarrow 0'} = \nu_1[\cos(\Gamma) + \sqrt{3}\sin(\Gamma)]\cos(2\pi\nu t),$$

$$\alpha_{1o\leftrightarrow 2o} = \nu_1\cos(2\pi\nu t). \tag{A7}$$

To summarize, the eigenstates $|i\rangle$ and eigenvalues E_i of $\mathcal{H}$ are

$$|2e'\rangle = \frac{\cos(\Gamma)}{\sqrt{2}}(|2\rangle + |-2\rangle) + \sin(\Gamma)|0\rangle, \quad E_{2e'} = 2\nu_q\sqrt{1+3\eta^2},$$

$$|1e\rangle = \frac{1}{\sqrt{2}}[|1\rangle + |-1\rangle], \quad E_{1e} = (3\eta-1)\nu_q,$$

$$|0'\rangle = \cos(\Gamma)|0\rangle - \frac{\sin(\Gamma)}{\sqrt{2}}(|2\rangle + |-2\rangle), \quad E_{0'} = -2\nu_q\sqrt{1+3\eta^2},$$

$$|1o\rangle = \frac{1}{\sqrt{2}}[|1\rangle - |-1\rangle], \quad E_{1o} = -(3\eta+1)\nu_q,$$

$$|2o\rangle = \frac{1}{\sqrt{2}}[|2\rangle - |-2\rangle], \quad E_{2o} = 2\nu_q, \tag{A8}$$

and an oscillating magnetic field $\vec{B}_1(t)$ can induce three transitions (see Fig. 4) at frequencies

$$\frac{\nu(|2e'\rangle \leftrightarrow |1e\rangle)}{\nu_q} = 2\sqrt{1+3\eta^2} + 1 - 3\eta \overset{\eta\ll 1}{\rightarrow} 3 - 3\eta,$$

$$\frac{\nu(|1e\rangle \leftrightarrow |0'\rangle)}{\nu_q} = 2\sqrt{1+3\eta^2} - 1 + 3\eta \overset{\eta\ll 1}{\rightarrow} 1 + 3\eta,$$

$$\frac{\nu(|1o\rangle \leftrightarrow |2o\rangle)}{\nu_q} = 3 + 3\eta. \tag{A9}$$

[1] C.P. Slichter, in *Principles of Magnetic Resonance*, 3rd ed. (Springer-Verlag, New York, 1990), pp. 485–500.

[2] H. Ackermann, P. Heitjans, and H.-J. Stöckmann, in *Hyperfine Interactions of Radioactive Nuclei*, edited by J. Christiansen, Topics in Current Physics Vol. 31 (Springer, Berlin, 1983), p. 291.

[3] B. Ittermann, G. Welker, F. Kroll, F. Mai, K. Marbach, and D. Peters, Phys. Rev. B **59**, 2700 (1999).

[4] P. Heitjans, W. Faber, and A. Schirmer, J. Non-Cryst. Solids **131**, 1053 (1991).

[5] R.F. Kiefl, G.D. Morris, P. Amaudruz, R. Baartman, J. Behr, J.H. Brewer, J. Chakhalian, S. Daviel, J. Doornbos, S.R. Dunsiger, S.R. Kreitzman, T. Kuo, C.D.P. Levy, R. Miller, M. Olivo, R. Poutissou, G.W. Wight, and A. Zelenski, Physica B **289–290**, 640 (2000).

[6] T.R. Beals, R.F. Kiefl, W.A. MacFarlane, K.M. Nichol, G.D. Morris, C.D.P. Levy, S.R. Kreitzman, R. Poutissou, S. Daviel, R.A. Baartman, and K.H. Chow, Physica B **326**, 205 (2003).

[7] R.F. Kiefl, W.A. MacFarlane, G.D. Morris, P. Amaudruz, D. Arseneau, H. Azumi, R. Baartman, T.R. Beals, J. Behr, C. Bommas, J.H. Brewer, K.H. Chow, E. Dumont, S.R. Dunsiger, S. Daviel, L. Greene, A. Hatakeyama, R.H. Heffner, Y. Hirayama, B. Hitti, S.R. Kreitzman, C.D.P. Levy, R.I. Miller, M. Olivo, and R. Poutissou, Physica B **326**, 189 (2003).

[8] A. Kastler, J. Phys. Radium **11**, 225 (1950); J. Brossel, A. Kastler, and J. Winter, *ibid.* **13**, 668 (1952); W.B. Hawkins and R.H. Dicke, Phys. Rev. **91**, 1008 (1953).

[9] M. Keim, U. Georg, A. Klein, R. Neugart, M. Neuroth, S. Wilbert, P. Lievens, L. Vermeeren, and the ISOLDE Collaboration, Hyperfine Interact. **97-98**, 543 (1996).

[10] C.D.P. Levy, A. Hatakeyama, Y. Hirayama, R.F. Kiefl, R. Baartman, J.A. Behr, H. Izumi, D. Melconian, G.D. Morris, R. Nussbaumer, M. Olivo, M. Pearson, R. Poutissou, and G.W. Wight, Nucl. Instrum. Methods Phys. Res. B **204**, 689 (2003).

[11] M.H. Cohen and F. Reif, Solid State Phys. **5**, 321 (1957).

[12] T.P. Das and E. L. Hahn, in *Nuclear Quadrupole Resonance Spectroscopy* (Academic, New York, 1958).

[13] W.A. MacFarlane, G.D. Morris, K.H. Chow, R.A. Baartman, S. Daviel, S.R. Dunsiger, A. Hatakeyama, S.R. Kreitzman, C.D.P. Levy, R.I. Miller, K.M. Nichol, R. Poutissou, E. Dumont, L.H. Greene, and R.F. Kiefl, Physica B **326**, 209 (2003).

[14] W. Körner, W. Keppner, B. Lehndorff-Junges, and G. Schatzet, Phys. Rev. Lett. **49**, 1735 (1982).

[15] O. Kanert, H. Schulz, and J. Albers, Solid State Commun. **91**, 465 (1994).

[16] Y. Inaguma, J.D. Yu, Y.J. Shan, M. Itoh, and T. Nakamura, J. Electrochem. Soc. **142**, L8 (1995); Y. Inaguma, Y. Matsui, Y.J. Shan, M. Itoh, and T. Nakamura, Solid State Ionics **79**, 91 (1995).